

**UT-TMB/MAT-LAM/Opti****Task Title: DEVELOPMENT OF NOVEL REDUCED ACTIVATION  
MARTENSITIC STEELS WITH IMPROVED CREEP PROPERTIES****INTRODUCTION**

A reduced activation martensitic ferritic Fe-9CrWTi alloy designed in a previous stage of the "Fusion" action [1], [2], and manufactured by Aubert et Duval, has been characterized, in terms of microstructure and precipitation kinetics. One of the main traits of this alloy is its reinforcement by MX precipitates, in this case, titanium carbides (TiC). Alongside with the characterization of the alloy, modelling of the precipitation kinetics and the microstructure evolution has been performed using MatCalc, a new suite of thermodynamics and kinetics software. MatCalc predictions show good agreement with experimental measurements on phase stability. Several semi-empirical methods have also been developed to monitor and characterize the microstructure evolution in this type of steels, based on physical properties like the martensite start temperature, thermoelectric power and hardness.

**2005 ACTIVITIES****Characterisation of titanium-strengthened alloy**

The characterization of a TiC reinforced reduced activation martensitic ferritic alloy with improved creep behaviour has been continued. Microstructural characterization is complete and mechanical characterization is underway [3]

The microstructure of this alloy confirms this strategy to obtain improved structural materials for application in fusion reactors and the suitability of this alloy for thin products. The heat treatments designed allow to develop a fine distribution of MX (TiC) precipitates that remain stable above the service temperature of the alloy and are expected to increase the creep resistance of the alloy without compromising its toughness.

However, the low quenchability of the family of alloys studied during this period suggests the need of a composition with higher quenchability for thick products.

**Assessment of thermodynamic/kinetic models and modelling TiC precipitation kinetics**

During this work, the characterization of the cast Fe9CrWTi has followed a parallel path of microstructural characterization and thermodynamic and kinetic modelling. MatCalc, a thermodynamics and kinetics package developed by Ernst KOZESCHNIK et al. [4],[5], at the Graz University of Technology (Austria) has been used to model the "as received" microstructure, and the TiC precipitation and dissolution reactions.

This model is specially suited for the description of precipitation reactions, allowing for the determination of the kinetics of reaction, fraction of precipitating phase, composition and size distribution of particles. It is also able to deal with simultaneous precipitation reactions in complex systems composed of many elements and containing multiple phases.

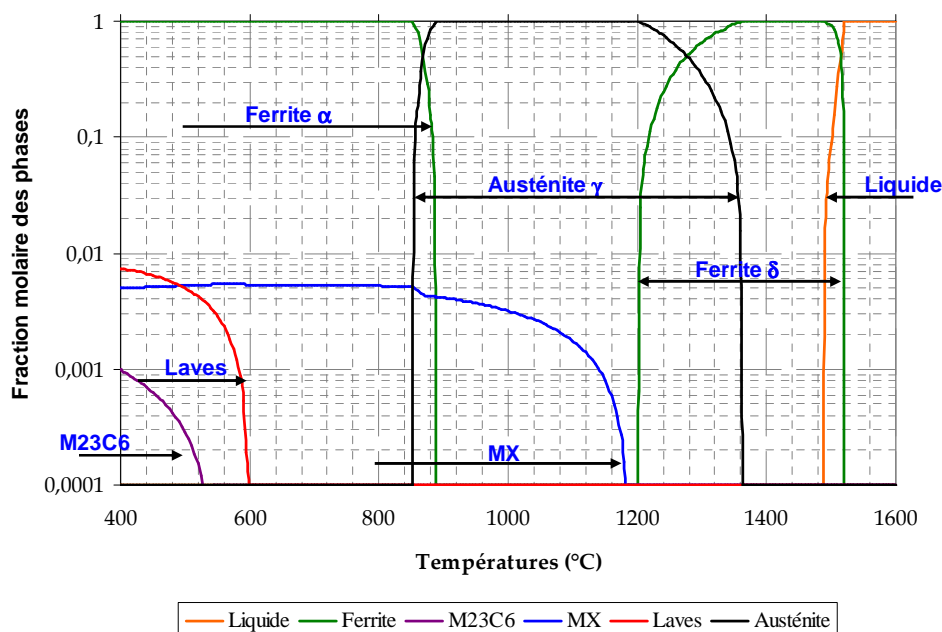


Figure 1: Phase stability diagram of Fe9CrWTi

The phase stability diagram for alloys of a standard Fe9CrWTi alloy has been calculated using MatCalc. Using this diagram, it is possible to design a heat treatment that will produce a microstructure with a fine and homogeneous dispersion of TiC precipitates this heat treatment includes austenitisation annealing at 1200°C during 30 minutes. During this annealing previous MX precipitates dissolve into the austenitic matrix. The solubilisation annealing is followed by a quench in oil ( $\dot{T} \approx -4^\circ\text{C}/\text{s}$ ) to create a martensitic structure. Finally, and in order to precipitate a very fine and homogeneous distribution of TiC, the alloy is tempered at 720°C for 10h. This tempering treatment leaves the martensitic structure basically unchanged, while it introduces the distribution of precipitates that will increase its stability. This temperature is also safely higher than the service temperature of the alloy (~650°C), and therefore it renders the alloy completely stable in service conditions.

To follow the nomenclature used at SMRA (CEA-Saclay), this heat treatment will be referred to as “AThR720”. A cast of an alloy Fe9CrWTi has been produced by the company Aubert & Duval, and provided in this condition. The alloy that has undergone such heat treatment is also referred to as “as received” material.

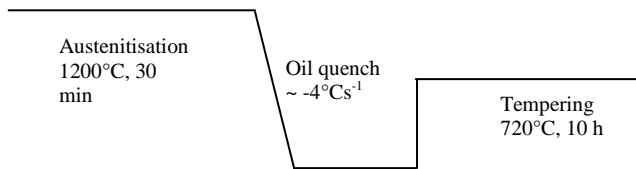


Figure 2: Schematic of the heat treatment AThR720

The simulation of the “as received” state of alloy Fe9CrWTi has allowed us to verify our expectations about its microstructure and evolution during successive heat treatments. It has been possible to predict that after the annealing at 1300°C for 30 minutes all carbides existing from the “as received” condition will have been dissolved.

The simulations also allow studying the complete dissolution of carbon and titanium during annealing at high temperature, and that the severity of the quench in oil is sufficient to keep most of those elements in solution.

During such quench, some TiC is formed, but of extremely fine size and in negligible mol fraction. During tempering at 720°C the precipitation of TiC reaches the equilibrium mole fraction, and the average size predicted is in good agreement with experimental measurements performed by small angle neutron scattering. Finally, of all possible precipitation reactions expected for this system, TiC is the most stable, in front of metastable cementite or  $M_{23}C_6$ .

To summarise, the simulation of heat treatments allows describing the transformation and precipitation reactions occurring during diverse heat treatments. By using a software package like MatCalc, it is possible to determine the mole fraction of precipitate phases, their number density, composition and size distribution.

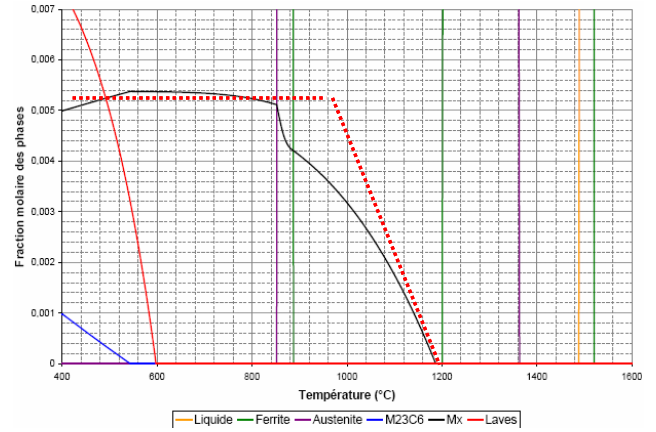


Figure 3: Phase stability diagram determined using MatCalc. The red dotted line describes the solubility of titanium carbides determined experimentally using indirect measurement techniques.

### Development of indirect methods to monitor precipitation reactions

The experimental and modelling study of the characterisation of the TiC solubilisation and precipitation processes in alloy Fe9CrWTi have shown that it is possible to describe and predict the microstructure obtained after a given heat treatment. However, it would also be of much value to be able to monitor the progress of such processes directly from the material properties, and ideally without the need of complex and time-consuming sample preparation.

In order to do that, the effect of precipitation (or degree of solubilisation) in the matrix have studied related to several different properties that could fit the requirements abovementioned. The temperature at which martensite transformation starts ( $M_S$ ), Hardness Vickers ( $H_V$ ) and Thermo-Electric Power measurements (TEP) are all parameters that are directly related to the composition of the matrix, and are simple to measure.

During the preliminary stages of this study hardness measurements have been ruled out due to the variability involved and their dependence on both the matrix composition and the morphology and distribution of precipitates. The relationships obtained are more elaborate versions of the ones obtained in Brachet [6]. The fact that we can consider the composition in carbon and titanium to vary hand in hand according to a close to stoichiometric ratio allows us to make the development described below. This development is shown for  $M_S$  but an analogous development can be followed for TEP.

$$\begin{cases} \Delta M_S^{MAX} = M_S - M_S^{ref} = K_{M_S}^C \cdot [\Delta C]_{\% wt} + K_{M_S}^{Ti} \cdot [\Delta Ti]_{\% wt} \\ \Delta PTE^{MAX} = PTE - PTE^{ref} = K_{PTE}^C \cdot [\Delta C]_{\% wt} + K_{PTE}^{Ti} \cdot [\Delta Ti]_{\% wt} \end{cases}$$

The fit between  $M_S$  and the annealing temperature is:  $M_S(^{\circ}\text{C}) = -0.2984 \cdot T(^{\circ}\text{C}) + 795.87$ . We can assume that all titanium carbides are dissolved after annealing at 1200°C and that all carbon and titanium are in solid solution in the matrix at this temperature.

On the other hand, the maximum fraction of precipitation (determined from the equilibrium phase diagram calculated with MatCalc) occurs between 720 and 860°C. The carbon and titanium contents of the matrix at those temperatures are negligible compared to the total content of each element in the alloy.

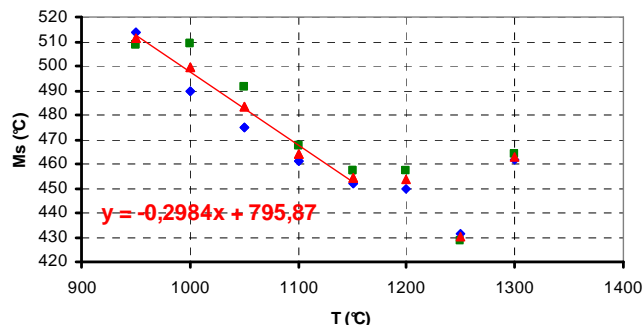


Figure 4: Fit of Ms temperature and annealing temperature.

Then, from the expression:

$$\Delta M_S^{MAX} = K_{M_S}^C \cdot [\Delta C]_{\% wt} + K_{M_S}^{Ti} \cdot [\Delta Ti]_{\% wt}$$

and using the coefficient for carbon determined by Brachet [5] ( $K_{M_S}^C = -600^\circ\text{C}/\text{wt}\%$ ), we arrive to the result that the coefficient for titanium is  $K_{M_S}^{Ti} = -277.5^\circ\text{C}/\text{wt}\%$ .

This equation allows therefore relating the matrix composition (and therefore the progress of precipitation) to a physical parameter easy to measure like  $M_S$ . A similar development can be performed with the thermo-electric power.

## CONCLUSIONS

A new family of reduced activation Fe9-12CrWTi martensitic alloys for fusion reactors has been developed and characterised. This type of alloys benefits on the reinforcing properties of a fine distribution of MX precipitates, in addition to M23C6 carbides used traditionally. This type of precipitates are more stable than M23C6 carbides used in alloys of the type EUROFER and others, and therefore the resulting alloy could have improved creep and toughness properties and to be able to work at higher service temperatures than the alloys used presently, up to 650°C for 10,000h.

During the development and characterisation of alloys Fe9CrWTi, substantial know-how in modelling of the microstructure using advanced thermodynamic, kinetic and statistic models has been developed, as well as semi-empirical models to monitoring its evolution.

In the next stages of this project, the approach of using a nanometric MX precipitates as additional reinforcing phase will be taken further in a new set of compositions that will lead to higher quenchability of the alloy and a more complex range of precipitating MX phases.

The line of compositions in which the main MX precipitate is a vanadium carbonitride will be prioritised over the alloys with TiC reinforcement phase.

## REFERENCES

- [1] Y. DE CARLAN, "Conception de nouveaux alliages ferritiques-martensitiques à activation réduite optimisés pour la résistance au fluage" Final Report UT-TBM/MAT-LAM/DES, CEA report, NT SRMA 03-2526, february 2003
- [4] E. KOZESCHNIK et al. "Modelling of kinetics in multi-component multi-phase systems with spherical precipitates. Part 1: Theory" & Part 2: Numerical solution and application" Materials science and engineering A, 385 (2004)
- [5] E. KOZESCHNIK et al. Modified evolution equations for the precipitation kinetics of complex phases in multi-component systems Computer coupling of phase diagrams and thermochemistry, 28 (2004)
- [6] J.C. BRACHET, "Correlation between thermoelectric power (TEP) and martensite start temperature (Ms) measurements of 9Cr-W-V-(Ta) martensitic steels", Journal de Physique IV, supplément au Journal de Physique III, Volume 5 (1995).

## REPORTS AND PUBLICATIONS

- [2] V. A. YARDLEY, 'Progress in Fabrication of Experimental 9Cr Steel Compositions Optimised for Creep Resistance, Proposed Solutions' CEA report, DMN/SRMA/LA2M/NT/04-2642/A
  - [3] D. GAUDE-FUGAROLAS, et Y. DE CARLAN, 'Intermediate report on the development of novel reduced activation martensitic steels with improved creep properties for fusion reactors' CEA report, DMN/SRMA/LA2M/NT/05-2751
- V. A. YARDLEY, Y. DE CARLAN, 'Design Criteria for High-Temperature Steels Strengthened with Vanadium Nitride', accepted for publication in special issue 'User Aspects of Phase Diagrams' of Journal of Phase Equilibria and Diffusion

## **TASK LEADER**

---

Yann de CARLAN

DEN/DMN/SRMA  
CEA-Saclay  
F-91191 Gif-sur-Yvette Cedex

Tel. : 33 1 69 08 61 75  
Fax : 33 1 69 08 71 30

e-mail : [yann.decarlan@cea.fr](mailto:yann.decarlan@cea.fr)

**UT-TBM/MAT-Micro****Task Title: MICROSTRUCTURAL EVOLUTION OF Fe-C MODEL ALLOY AND EUROFER UNDER 1 MeV ELECTRON IRRADIATION WITH AND WITHOUT He PRE-IMPLANTATION****INTRODUCTION**

A multiscale modelling programme has been initiated whose ultimate aim is to study the radiation effects in the Eurofer ferritic/martensitic steel in the presence of high concentrations of nuclear derived impurities [1].

The development of these models requires an experimental validation and, in the case of complex multicomponent industrial alloys such as Eurofer, the values of model parameters will have to be tuned based on experimental data. Although many microstructural investigations following irradiation experiments of steels, including Eurofer, have been carried out in the past, the data are not adequate for model validation because the irradiation conditions are often complex and/or not well known.

We have therefore proposed to perform parametric irradiation experiments of a model Fe-C alloy and Eurofer, under well controlled conditions (temperature, dose, damage rate), using 1 MeV electrons with and without helium pre-implantation. 1 MeV electrons create only isolated defects (Frenkel pairs) in steels, i.e. the primary damage is perfectly well known, which is an additional advantage in view of the comparison with model predictions.

**2005 ACTIVITIES**

In 2005, it was intended to perform 1 MeV electron irradiation experiments of Eurofer at different temperatures using the 1 MV High Voltage Electron Microscope (EM7 AEI/KRATOS microscope) located at CEA-Saclay.

The goal was to characterize by Transmission Electron Microscopy (TEM) the irradiation-induced point defect clusters and in particular the number densities at saturation of interstitial dislocation loops. Similar experiments have been carried out in the past on a Fe-C model alloy containing 20 wtppm carbon [2].

As the microstructure of Eurofer in the standard metallurgical condition (Normalized and tempered), which consists of fine martensite laths containing a high dislocation density, would complicate the measurements of number densities of tiny dislocation loops, we have first applied a specific heat treatment, in order to obtain a 100% ferritic metallurgical condition. This heat treatment, which basically consisted of an isothermal decomposition of austenite into ferrite, is schematically described in figure 1.

Following the heat treatment, optical microscopy as well as hardness measurements confirmed that a fully ferritic structure had been obtained. Discs 3 mm in diameter were then punched out from a heat-treated Eurofer specimen mechanically polished down to a thickness of 100  $\mu\text{m}$  and were subsequently electropolished to prepare thin foils suitable for TEM investigations.

The thin foils were irradiated with 1 MeV electrons in the HVEM using a heating specimen holder. The irradiation experiments were performed at three temperatures (360, 290 and 210°C) with a damage rate of  $6 \cdot 10^{-4}$  dpa/s and up to a maximum dose of about 0.8 dpa.

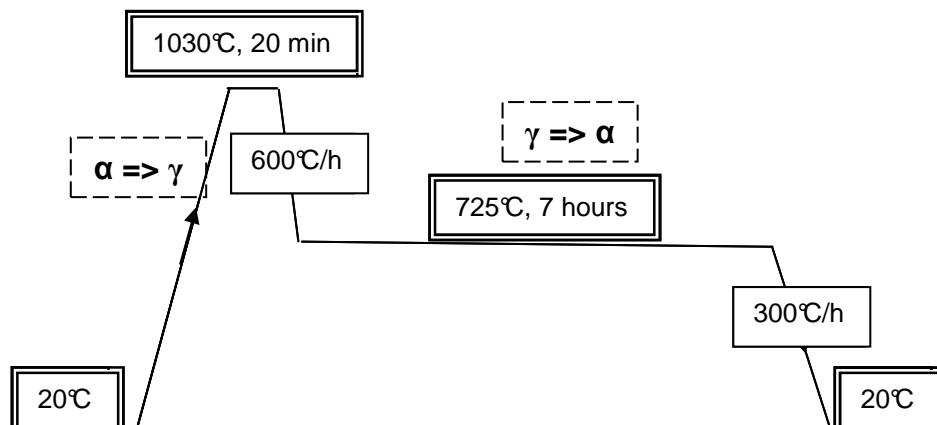
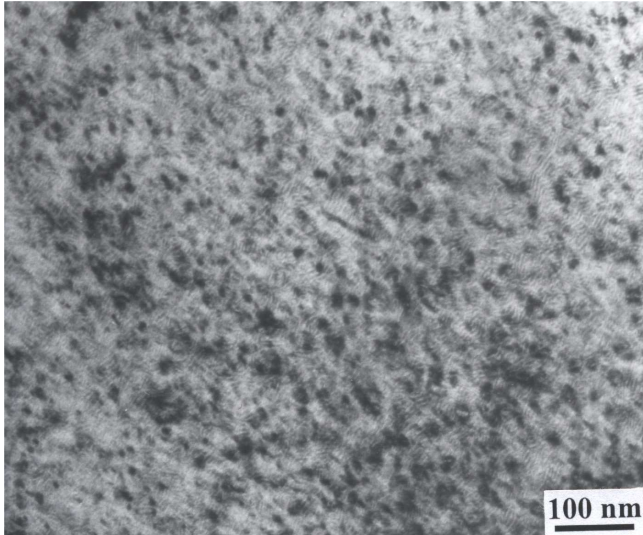


Figure 1: Heat treatment applied to the Eurofer steel in order to obtain a fully ferritic metallurgical condition.

Following the irradiation experiments, the specimens were characterized in a conventional TEM operated at 200kV.

A representative micrograph of the microstructure induced by irradiation at 210°C is shown in figure 2.



*Figure 2: Microstructure of ferritic Eurofer steel irradiated with 1 MeV electrons at 210°C (0.8 dpa). Kinematical bright field imaging conditions with  $g = \{110\}$ .*

This microstructure consists of a high density of small dislocation loops. Unfortunately, during the experiments, the vacuum in the vicinity of the specimen could not be kept at a suitable value, presumably due to a microleak. As a result, oxidation/contamination of the samples occurred, as evidenced for instance by the numerous moiré fringes which can be seen on the TEM micrograph (figure 2). This phenomenon was even more pronounced at the higher irradiation temperatures. It is therefore not possible to use the presently irradiated specimens to obtain reliable quantitative data on the microstructural evolution of Eurofer under electron irradiation. Work is in progress to localize and suppress the microleak presumably causing the oxidation, so that a new series of experiments can be carried out.

## CONCLUSIONS

---

Following a specific heat treatment performed in order to obtain a fully ferritic condition, Eurofer specimens were irradiated in the Saclay HVEM with 1 MeV electrons at different temperatures. However, the subsequent characterization in a 200 kV TEM showed that the irradiated samples were significantly oxidized due to a vacuum problem in the HVEM. A new irradiation campaign will be carried out once this problem is solved. Thereafter, room temperature implantations to a low helium concentration of Eurofer and Fe-C samples will be performed, followed by electron irradiations in order to assess the effect of helium on point defect clustering in both materials.

## REFERENCES

---

- [1] M. Victoria, G. Martin, B. Singh, The role of the modelling of irradiation effects in metals in the European Fusion Materials Long Term Program.
- [2] A. Hardouin Duparc, C. Moingeon, N. Smetniansky-de-Grande, A. Barbu, J. Nucl. Mater. 302 (2002) 143

## TASK LEADER

---

Jean HENRY

DEN/DMN/SRAM/LA2M  
CEA-Saclay  
F-91191 Gif-sur-Yvette Cedex

Tel. : 33 1 69 08 85 08  
Fax : 33 1 69 08 71 30

e-mail : jean.henry@cea.fr

**UT-TBM/MAT-Modpulse****Task Title: PULSED IRRADIATION OF THE MARTENSITIC ALLOY EUROFER****INTRODUCTION**

In the framework of the study of irradiation microstructures in ferritic stainless steel, the purpose is to investigate the secondary defects distribution to test the influence of the irradiation mode. Three modes are experimented at the same damage (3 dpa). Two modes are long time irradiations: cyclic (pulsed), and continuous. The third is a short time irradiation reported last year. The results in Eurofer are compared to irradiations in a model alloy.

**2005 ACTIVITIES****MATERIAL AND IRRADIATION CONDITIONS**

The Eurofer97 (table 1) is delivered by SRMA (A. Alamo), [1].

The model ferritic alloy (Fe/9% w. Cr) is elaborated at the SRMP by high frequency heating of high purity Fe (99.999%) and Cr (99.99%).

In the Eurofer, the microstructure is very similar from one foil to the other. It consists in laths containing a high density of dislocations. The model alloy is fully ferritic and only scarce dislocation lines are visible at the microscope scale.

This year, long time irradiations at the same aimed fluence have been performed in the Van de Graaff accelerator of the SRMP (table 2). The samples are irradiated as disks for transmission electron microscope holders (diameter: 3 mm) extracted from the foil by punching. Then, they are thinned in a double jet device (Tenupol 2 from STRUERS).

**IRRADIATION MICROSTRUCTURE****Irradiation at 350°C**

Inside the lath microstructure of Eurofer, dislocation loops are observed as large defects (max 22 nm) and black dots. Due to the bending of the foils, the observation is limited to a small region close to the extinction fringes and the better images are given by bright field conditions (figure 1). A histogram of the sizes distribution has been obtained, which shows two populations of loops (figure 3). One peaks around 7 nm and the second around 19 nm.

In the model alloy, a similar microstructure is present (figure 2). Again, loops are present with a bi-modal distribution (figure 4) but the density is larger with a factor about 1.5. The high density of loops impedes a safe loop size histogram. Some loops are very large (> 30 nm) and some dislocation lines are present.

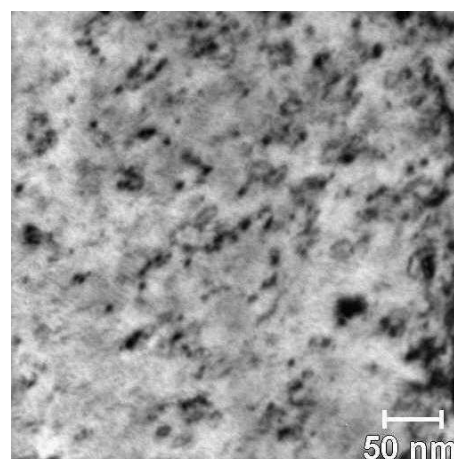


Figure 1: Eurofer irradiated at 350°C

Table 1: Chemical composition of Eurofer97

element	C	Cr	W	Ta	V	Mn	Si	Ni	N	Nb
weight percent	0.12	8.96	1.04	0.15	0.18	0.48	0.03	0.06	0.022	<0.002

Table 2: Irradiation conditions aimed

ion	Energy	Damage	Fluence	Time	dpa/s
Kr <sup>++</sup>	700 keV	3 dpa	$9.64 \cdot 10^{14}$ ions.cm <sup>-2</sup>	6 h	$2.8 \cdot 10^{-3}$

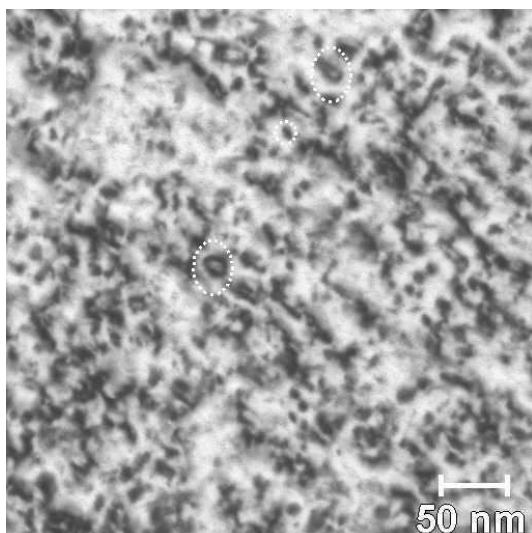


Figure.2: Model alloy irradiated at 350°C

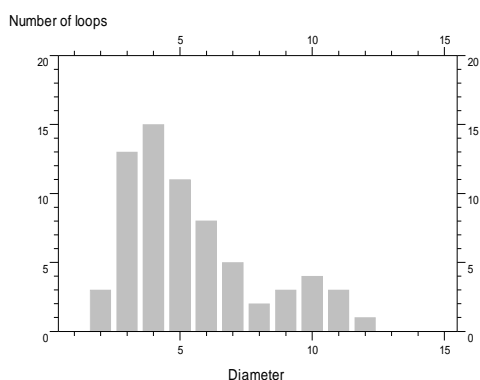


Figure 3: Eurofer, distribution of the loops size after irradiation at 350°C

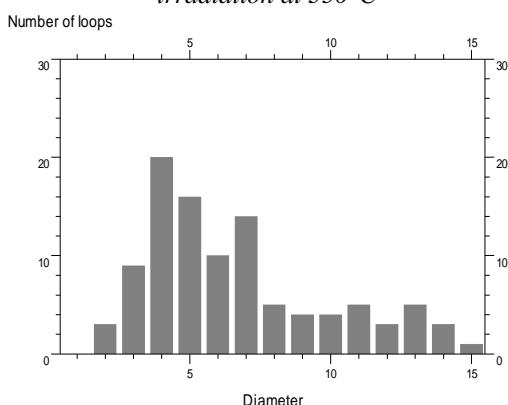


Figure 4: Model alloy, distribution of the loops size after irradiation at 350°C

**Discrepancies at 350°C with short time irradiations**

One major difference is the lack of clusters in the Eurofer after short time relatively to the presence of clusters after long time (table 3). This absence has been analysed by heating the sample at higher temperature: 550°C. The formation of defects has been observed, meaning that the clusters were too small to be observed at that fluence.

The larger fluence of the long time irradiation is the main argument to explain the formation of loops in the Eurofer. The population of loops present a bi-modal distribution with two peaks at 7 and 19 nm.

In the model alloy, as compared to short time irradiations, the loop size increases and again a bi-modal distribution is present.

**Irradiation at 550°C**

At this temperature, both oxidation and dense microstructure make the observation inside the laths more difficult. Only a few regions are available to give good images (figure 5). In this case, large defects located in {100} are present as dislocation loops (> 80 nm).

The model alloy shows less deformation of the grains, which allows the realization of better pictures than in the

Eurofer. It presents a homogeneous distribution of loops with a density of  $1-2 \cdot 10^{20} \text{ m}^{-3}$ . figure 6 presents these loops when they are seen edge on. Their density forbids observations of other defects.

These loops are shown for the best when they are seen edge on. They are mainly located in {100} planes but some of them are shown in planes closed to {~120}. The diameter of these loops reaches the large value of 400 nm with a mean value around 200 nm.

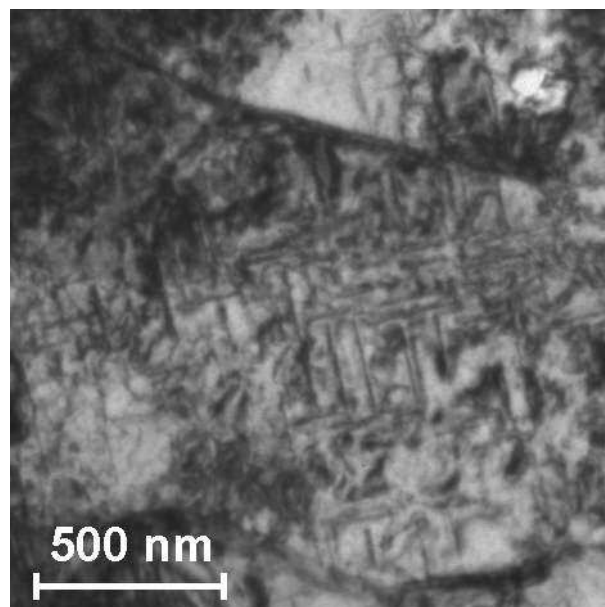


Figure 5: Eurofer irradiated at 550°C : loops edge on inside a martensitic lath

Table 3: Microstructure at 350°C after short and long time irradiation

		Eurofer	Model alloy
Short time	Loops density	no observable defects	uni-modal distribution : $\sim 5 \cdot 10^{21} \text{ m}^{-3}$
	Loops size	-	small loops : $< 5 \text{ nm}$
Long time	Loops density	about twice than in the model alloy $\sim 3 \cdot 10^{21} \text{ m}^{-3}$	bi-modal distribution: $\sim 5 \cdot 10^{21} \text{ m}^{-3}$
	Loops size	two sizes : 7 and 19 nm	larger loops, two sizes : 7 and 28 nm

Table 4: Microstructure at 550°C after short and long time irradiation

		Eurofer	Model alloy
Short time	Loops density	heterogeneous, $< 10^7 \cdot \text{m}^{-1}$ ,	$< 10^{20} \text{ m}^{-3}$
	Loops size	max 150 nm	max 150 nm
Long time	Loops density	at least twice larger than after short time	$1-2 \cdot 10^{20} \text{ m}^{-3}$
	Loops size	max 300 nm	max 400 nm

**Discrepancies at 550°C with short time irradiations**

The same type of larges loops are present after short and long time irradiation in the two alloys (table 4). After long time irradiation, the clusters are very much larger with a higher density. Too much defects are present to give a good observation.

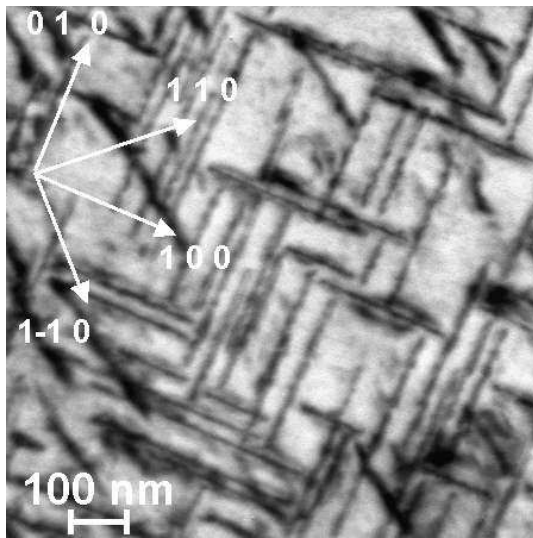


Figure 6: Model alloy irradiated at 550°C : loops in 100 and ~120 planes

The original dislocation network is still visible between loops after short time irradiation in Eurofer. It is no more possible to observe it after the long time irradiation.

**CONCLUSIONS**

At 350°C, in Eurofer and the model alloy, the loops are very much smaller relatively to the ones present after

irradiation at 550°C. In the two materials a bi-modal distribution is present. This difference with fcc metals needs to be cleared [2]. The lack of defects, at 350°C, in Eurofer, after short time irradiation is attributed to a realized fluence lower than after long time irradiation.

At 550°C, long time, the loops are very much larger than after short time. Again, the obtained fluence was too high. Nevertheless the size of loops at 550°C is too large, meaning that a lower damage may be sufficient. There is no loops free zone (LFZ) close to the laths interfaces and in thin region the LFZ is limited.

As a comparison with short time irradiations, the larger densities and sizes of loops that are present after long time irradiation are attributed to an unexpected higher damage. For future irradiations, a more controlled fluence is wished. It is unlikely that a flux effect would give a such tendency.

In the two alloys, the microstructure is similar. Consequently, the martensitic structure as well as the minors alloy elements does not influence the loop microstructure in the Eurofer.

**REFERENCES**

---

[1] Metallurgical characterization of as-received Eurofer97 products, C. A. Danon, S. Urvoy, A. Alamo CEA report, NT SRMA 01-2418, march 2001.

[2] Interstitial loops configurations after two modes of pulsed and monotonous irradiation at 600, 370 and 200°C, comparison with high flux continuous irradiation. Origin of the erratic formation of scarce voids. L. Boulanger and Y. Serruys, CEA report, NT DEN/SAC/DMN/SRMP 2003-01

## **REPORTS AND PUBLICATIONS**

---

Preparation of Eurofer samples for pulsed irradiations,  
L. Boulanger and Y. Serruys, CEA report, NT  
DEN/SAC/DMN/SRMP 2004-01

Monotonous short time irradiation of Eurofer at 350 and  
550°C, L. Boulanger and Y. Serruys, CEA report, NT  
DEN/SAC/DMN/SRMP 2004-012

Annealing of Eurofer irradiated at 350°C,  
L. Boulanger and Y. Serruys, CEA report, NT  
DEN/SAC/DMN/SRMP 2005-04

Annealing of Eurofer irradiated at 350°C,  
L. Boulanger and Y. Serruys, CEA report, NT  
DEN/SAC/DMN/SRMP 2005-20

## **TASK LEADER**

---

Loic BOULANGER

DEN/DMN/SRMP  
CEA-Saclay  
F-91191 Gif-sur-Yvette Cedex

Tel. : 33 1 69 08 64 19  
Fax : 33 1 69 08 68 67

e-mail : loic.boulanger@cea.fr